4 Axial Surface Waves in Isotropic Media

4.1 Definition

An axial surface wave is a plane wave that propagates in the axial direction of a cylindrical interface of two different media without radiation.

Axial surface waves are plane waves because the phase remains constant along a plane perpendicular to the cylinder axis. They are also inhomogeneous because the field is not constant along surfaces of constant phase.

A study of axial surface waves has been included in this text because this type of waves may be the cause of some significant contributions to the RCS of an aircraft. Axial surface waves can propagate along the body of a coated missile (13 in Fig. 1.5) and also the waves that propagate along the trailing edge of a coated wing (14 in Fig. 1.5) very much resemble these axial surface waves.

Sommerfeld was first to suggest the existence of axial surface waves in 1899. Goubau subsequently developed the idea in its application to a transmission line consisting of a coated metal wire (Fig. 4.1) [1]. With reference to this early research, the terms *Sommerfeld wave* and *Goubau wave* are sometimes used to denote an axial surface wave along a homogeneous rod and a coated metal wire, respectively. Axial surface waves are perhaps the most important type of surface waves with regard to practical applications [2]. Not only the Goubau line of Figure 4.1, but also the polyrod antenna supports axial surface waves [3].

Formulas for the electromagnetic field components in function of a Hertz potential were found in Section 2.6. Moreover, (2.30) and (2.31) appear to imply that the longitudinal components of $\vec{E}$ and $\vec{H}$ are uncoupled, as was the case with the plane surface waves discussed in Chapter 3. However, in general, coupling of the longitudinal field components E_z and H_z is required by the boundary conditions of the electromagnetic field components [4, p.38]. This is in contrast with plane surface waves where the boundary conditions do not lead to coupling between the field components, resulting in mode solutions for which the longitudinal component of either $\vec{E}$ or $\vec{H}$ is zero. These modes were called H-type (TE) and E-type (TM), respectively. Cylindrical interfaces, however, not only support pure TE and TM axial surface wave modes but also modes for which both E_z and H_z are nonzero. These latter modes are in fact combinations of a TE and TM mode with a same β_z and are therefore called *hybrid modes*. They are designated as EH or HE modes, depending on whether the TM or the TE mode predominates, respectively [5, p. 721]. Representations of the field distributions of these different types of axial surface wave modes can be found at the end of this chapter.

4.2 Axial Surface Waves along a Coated, Electric Perfectly Conducting Cylinder

The propagation of axial surface waves along a uniformly coated PEC cylinder will be analysed in this section. The structure under investigation actually corresponds to the Goubau line (Fig. 4.1).

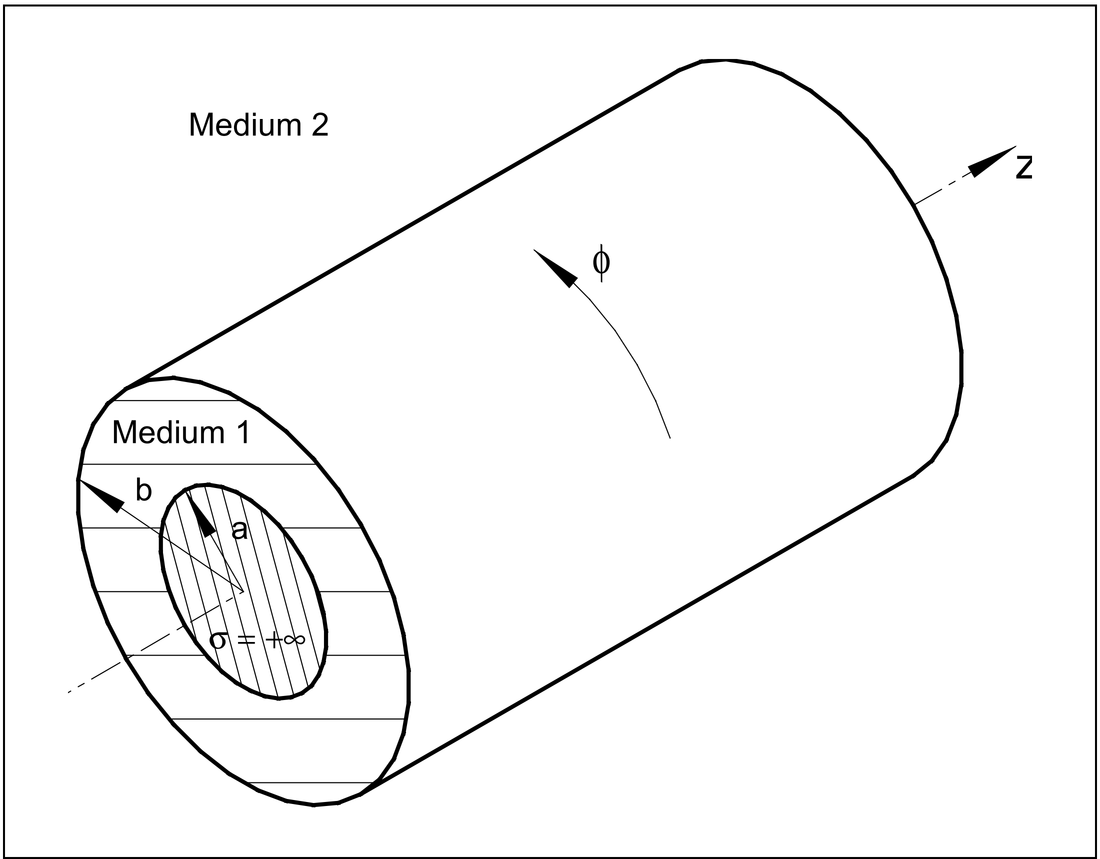

Figure 4.1: A uniformly coated PEC cylinder (Goubau line)

As was pointed out earlier, a cylindrical interface can support hybrid modes in addition to the pure TM and TE modes. In order to obtain hybrid mode solutions, equations (2.30) and (2.31) need to be evaluated simultaneously which makes the analysis more complex than the analysis of plane surface waves.

Suitable Hertz functions for medium 1 that can satisfy the boundary conditions $E_z = 0$ and $E_\phi = 0$ at $r = a$ are

$$\Pi_{1e} = \sum_n \left[A_{1J_n} J_n(s_{r1}r) + A_{1Y_n} Y_n(s_{r1}r)\right] e^{-jn\phi} e^{-j\beta_z z} \text{ and} \tag{1}$$

$$\Pi_{1m} = \sum_n \left[B_{1J_n} J_n(s_{r1}r) + B_{1Y_n} Y_n(s_{r1}r)\right] e^{-jn\phi} e^{-j\beta_z z} \tag{2}$$

where n is a positive integer.
Because of their similarity to harmonic functions and their oscillatory behaviour, the Bessel functions J_n and Y_n may be interpreted here as standing waves in the r-direction.

Substituting (1) and (2) into (2.30) and (2.31), respectively, gives

$$E_{z1} = s_{r1}^2 \sum_n \left[A_{1J_n} J_n(s_{r1}r) + A_{1Y_n} Y_n(s_{r1}r)\right] e^{-jn\phi} e^{-j\beta_z z}, \tag{3a}$$

$$E_{r1} = \sum_n \left[-j\beta_z s_{r1}\left[A_{1J_n} J_n'(s_{r1}r) + A_{1Y_n} Y_n'(s_{r1}r)\right] - \frac{n\omega\mu_1}{r}\left[B_{1J_n} J_n(s_{r1}r) + B_{1Y_n} Y_n(s_{r1}r)\right]\right] e^{-jn\phi} e^{-j\beta_z z}, \tag{3b}$$

$$E_{\phi 1} = \sum_n \left[-\frac{n\beta_z}{r}\left[A_{1J_n} J_n(s_{r1}r) + A_{1Y_n} Y_n(s_{r1}r)\right] + j\omega\mu_1 s_{r1}\left[B_{1J_n} J_n'(s_{r1}r) + B_{1Y_n} Y_n'(s_{r1}r)\right]\right] e^{-jn\phi} e^{-j\beta_z z}, \tag{3c}$$

$$H_{z1} = s_{r1}^2 \sum_n \left[B_{1J_n} J_n(s_{r1}r) + B_{1Y_n} Y_n(s_{r1}r)\right] e^{-jn\phi} e^{-j\beta_z z}, \tag{3d}$$

$$H_{r1} = \sum_n \left[-j\frac{n(\sigma_1 + j\omega\varepsilon_1)}{r}\left[A_{1J_n} J_n(s_{r1}r) + A_{1Y_n} Y_n(s_{r1}r)\right] - j\beta_z s_{r1}\left[B_{1J_n} J_n'(s_{r1}r) + B_{1Y_n} Y_n'(s_{r1}r)\right]\right] e^{-jn\phi} e^{-j\beta_z z}, \tag{3e}$$

$$H_{\phi 1} = \sum_n \left[-(\sigma_1 + j\omega\varepsilon_1) s_{r1}\left[A_{1J_n} J_n'(s_{r1}r) + A_{1Y_n} Y_n'(s_{r1}r)\right] - \frac{n\beta_z}{r}\left[B_{1J_n} J_n(s_{r1}r) + B_{1Y_n} Y_n(s_{r1}r)\right]\right] e^{-jn\phi} e^{-j\beta_z z}. \tag{3f}$$

Bessel functions of the second kind (Y_n) are not defined for negative real arguments. Hence,

$$s_{r1} = \operatorname{sign}\left[\operatorname{Re}\left(\sqrt{k_1^2 - \beta_z^2}\right)\right]\sqrt{k_1^2 - \beta_z^2}. \tag{4}$$

Large argument approximations for J_n and Y_n are [5, p. 835], [6, p. 228]

$$J_n(x) \approx \sqrt{\frac{2}{\pi x}} \cos\left(x - \frac{\pi}{4} - n\frac{\pi}{2}\right) \text{ and} \tag{5}$$

$$Y_n(x) \approx \sqrt{\frac{2}{\pi x}} \sin\left(x - \frac{\pi}{4} - n\frac{\pi}{2}\right), \text{ both for } |x| >> 1. \tag{6}$$

Suitable Hertz functions for medium 2 that satisfy the boundary condition $\vec{E} = \vec{H} = \vec{0}$ when $r \to +\infty$
are

$$\Pi_{2e} = \sum_n A_2 H_n^{(2)}(s_{r2} r) e^{-jn\phi} e^{-j\beta_z z} \text{ and} \tag{7}$$

$$\Pi_{2m} = \sum_n B_2 H_n^{(2)}(s_{r2} r) e^{-jn\phi} e^{-j\beta_z z} . \tag{8}$$

The reason why Hankel functions of the second kind are used instead of those of the first kind, becomes clear by looking at the large argument approximations of both function types. These are [5, p. 835] and [6, p. 228]

$$H_n^{(1)}(x) \approx \sqrt{\frac{2}{\pi x}} e^{j\left(x - \frac{\pi}{4} - n\frac{\pi}{2}\right)} \text{ and} \tag{9}$$

$$H_n^{(2)}(x) \approx \sqrt{\frac{2}{\pi x}} e^{-j\left(x - \frac{\pi}{4} - n\frac{\pi}{2}\right)}, \text{ both for } |x| >> 1. \tag{10}$$

Comparing (9) and (10) with the equivalent Hertz potentials for plane surface waves (3.7) and (3.18) and following the same reasoning as in Sections 3.4.2 and 3.4.3 leads to the following conclusions:

- the use of Hankel functions of the second kind in Hertz potentials gives rise to proper axial wave solutions,
- whereas using Hankel functions of the first kind results in improper axial wave solutions.

It is also important to know that Hankel functions are undefined for negative pure real numbers [7]. However, when the imaginary part of the argument is nonzero, the real part can have any value. Hence, for proper axial waves (see also (3.8) and (3.19) and Appendix 3.B)

$$s_{r2} = \text{sign}\left[\text{Re}\left(\sqrt{k_2^2 - \beta_z^2}\right)\right]\sqrt{k_2^2 - \beta_z^2} \;\Rightarrow\; js_{r2} = \text{sign}\left[\text{Re}\left(\sqrt{\beta_z^2 - k_2^2}\right)\right]\sqrt{\beta_z^2 - k_2^2} , \tag{11a}$$

whereas for improper axial waves

$$s_{r2} = -\text{sign}\left[\text{Re}\left(\sqrt{k_2^2 - \beta_z^2}\right)\right]\sqrt{k_2^2 - \beta_z^2} \;\Rightarrow\; js_{r2} = -\text{sign}\left[\text{Re}\left(\sqrt{\beta_z^2 - k_2^2}\right)\right]\sqrt{\beta_z^2 - k_2^2} . \tag{11b}$$

Substituting (7) and (8) into (2.30) and (2.31), respectively, gives

$$E_{z2} = s_{r2}^2 \sum_n A_2 H_n^{(2)}(s_{r2} r) e^{-jn\phi} e^{-j\beta_z z} , \tag{12a}$$

$$E_{r2} = \sum_n \left[-j\beta_z A_2 s_{r2} H_n'^{(2)}(s_{r2} r) - \frac{n\omega\mu_2}{r} B_2 H_n^{(2)}(s_{r2} r) \right] e^{-jn\phi} e^{-j\beta_z z} , \tag{12b}$$

$$E_{\phi 2} = \sum_n \left[-\frac{n\beta_z}{r} A_2 H_n^{(2)}(s_{r2} r) + j\omega\mu_2 B_2 s_{r2} H_n'^{(2)}(s_{r2} r) \right] e^{-jn\phi} e^{-j\beta_z z} , \tag{12c}$$

$$H_{z2} = s_{r2}^2 \sum_n B_2 H_n^{(2)}(s_{r2} r) e^{-jn\phi} e^{-j\beta_z z} , \tag{12d}$$

$$H_{r2} = \sum_n \left[-j\frac{n(\sigma_2 + j\omega\varepsilon_2)}{r} A_2 H_n^{(2)}(s_{r2} r) - j\beta_z B_2 s_{r2} H_n'^{(2)}(s_{r2} r) \right] e^{-jn\phi} e^{-j\beta_z z} , \tag{12e}$$

$$H_{\phi 2} = \sum_n \left[-(\sigma_2 + j\omega\varepsilon_2) A_2 s_{r2} H_n'^{(2)}(s_{r2} r) - \frac{n\beta_z}{r} B_2 H_n^{(2)}(s_{r2} r) \right] e^{-jn\phi} e^{-j\beta_z z} . \tag{12f}$$

The tangential components of $\vec{E}$ must vanish at the surface of the perfect electric conductor.

$E_{z1} = 0$ at $r = a$

$$\Rightarrow \; A_{1Y_n} = -\frac{J_n(s_{r1}a)}{Y_n(s_{r1}a)} A_{1J_n} \text{ and} \tag{13}$$

$E_{\phi 1} = 0$ at $r = a$ gives, by virtue of (3c) and (13),

$$B_{1Y_n} = -\frac{J_n'(s_{r1}a)}{Y_n'(s_{r1}a)} B_{1J_n}. \tag{14}$$

The tangential components of both $\vec{E}$ and $\vec{H}$ are continuous across the interface of two media. This gives, by virtue of (13) and (14)

$E_{z1} = E_{z2}$ at $r = b$

$$\Rightarrow \; s_{r1}^2\left[J_n(s_{r1}b) - \frac{J_n(s_{r1}a)}{Y_n(s_{r1}a)} Y_n(s_{r1}b)\right] A_{1J_n} - s_{r2}^2 H_n^{(2)}(s_{r2}b) A_2 = 0, \tag{15}$$

$E_{\phi 1} = E_{\phi 2}$ at $r = b$

$$\begin{aligned}\Rightarrow \; & -\frac{n\beta_z}{b}\left[J_n(s_{r1}b) - \frac{J_n(s_{r1}a)}{Y_n(s_{r1}a)} Y_n(s_{r1}b)\right] A_{1J_n} \\ & + j\omega\mu_1 s_{r1}\left[J_n'(s_{r1}b) - \frac{J_n'(s_{r1}a)}{Y_n'(s_{r1}a)} Y_n'(s_{r1}b)\right] B_{1J_n} \\ & + \frac{n\beta_z}{b} H_n^{(2)}(s_{r2}b) A_2 - j\omega\mu_2 s_{r2} H_n'^{(2)}(s_{r2}b) B_2 = 0,\end{aligned} \tag{16}$$

$H_{z1} = H_{z2}$ at $r = b$

$$\Rightarrow \; s_{r1}^2\left[J_n(s_{r1}b) - \frac{J_n'(s_{r1}a)}{Y_n'(s_{r1}a)} Y_n(s_{r1}b)\right] B_{1J_n} - s_{r2}^2 H_n^{(2)}(s_{r2}b) B_2 = 0 \tag{17}$$

and finally $H_{\phi 1} = H_{\phi 2}$ at $r = b$

$$\begin{aligned}\Rightarrow \; & -(\sigma_1 + j\omega\varepsilon_1) s_{r1}\left[J_n'(s_{r1}b) - \frac{J_n(s_{r1}a)}{Y_n(s_{r1}a)} Y_n'(s_{r1}b)\right] A_{1J_n} \\ & - \frac{n\beta_z}{b}\left[J_n(s_{r1}b) - \frac{J_n'(s_{r1}a)}{Y_n'(s_{r1}a)} Y_n(s_{r1}b)\right] B_{1J_n} \\ & + (\sigma_2 + j\omega\varepsilon_2) s_{r2} H_n'^{(2)}(s_{r2}b) A_2 + \frac{n\beta_z}{b} H_n^{(2)}(s_{r2}b) B_2 = 0.\end{aligned} \tag{18}$$

Equations (15), (16), (17) and (18) form a system of linear equations for the four unknown factors A_{1J_n}, B_{1J_n}, A_2 and B_2. The system is homogeneous, hence for non-trivial solutions to exist, the coefficient determinant must be zero, that is

$$\begin{vmatrix} s_{r1}^2\left[J_n(s_{r1}b)-\frac{J_n(s_{r1}a)}{Y_n(s_{r1}a)}Y_n(s_{r1}b)\right] & 0 & -s_{r2}^2H_n^{(2)}(s_{r2}b) & 0 \\ -\frac{n\beta_z}{b}\left[J_n(s_{r1}b)-\frac{J_n(s_{r1}a)}{Y_n(s_{r1}a)}Y_n(s_{r1}b)\right] & j\omega\mu_1 s_{r1}\left[J_n'(s_{r1}b)-\frac{J_n'(s_{r1}a)}{Y_n'(s_{r1}a)}Y_n'(s_{r1}b)\right] & \frac{n\beta_z}{b}H_n^{(2)}(s_{r2}b) & -j\omega\mu_2 s_{r2}H_n'^{(2)}(s_{r2}b) \\ 0 & s_{r1}^2\left[J_n(s_{r1}b)-\frac{J_n'(s_{r1}a)}{Y_n'(s_{r1}a)}Y_n(s_{r1}b)\right] & 0 & -s_{r2}^2H_n^{(2)}(s_{r2}b) \\ -(\sigma_1+j\omega\varepsilon_1)s_{r1}\left[J_n'(s_{r1}b)-\frac{J_n(s_{r1}a)}{Y_n(s_{r1}a)}Y_n'(s_{r1}b)\right] & -\frac{n\beta_z}{b}\left[J_n(s_{r1}b)-\frac{J_n'(s_{r1}a)}{Y_n'(s_{r1}a)}Y_n(s_{r1}b)\right] & (\sigma_2+j\omega\varepsilon_2)s_{r2}H_n'^{(2)}(s_{r2}b) & \frac{n\beta_z}{b}H_n^{(2)}(s_{r2}b) \end{vmatrix} = 0. \tag{19}$$

Expanding the above determinant does not result in a simplified expression. Equation (19) may therefore be regarded as the dispersion equation of the axial surface waves propagating along a Goubau line.

However, it can be shown that, for n=0, (19) reduces to

$$\left[(\sigma_1+j\omega\varepsilon_1)s_{r2}\left[J_0'(s_{r1}b)-\frac{J_0(s_{r1}a)}{Y_0(s_{r1}a)}Y_0'(s_{r1}b)\right]H_0^{(2)}(s_{r2}b)-(\sigma_2+j\omega\varepsilon_2)s_{r1}\left[J_0(s_{r1}b)-\frac{J_0(s_{r1}a)}{Y_0(s_{r1}a)}Y_0(s_{r1}b)\right]H_0'^{(2)}(s_{r2}b)\right]$$
$$\cdot\left[j\omega\mu_1 s_{r2}\left[J_0'(s_{r1}b)-\frac{J_0'(s_{r1}a)}{Y_0'(s_{r1}a)}Y_0'(s_{r1}b)\right]H_0^{(2)}(s_{r2}b)-j\omega\mu_2 s_{r1}\left[J_0(s_{r1}b)-\frac{J_0'(s_{r1}a)}{Y_0'(s_{r1}a)}Y_0(s_{r1}b)\right]H_0'^{(2)}(s_{r2}b)\right]=0. \tag{20}$$

Also, for n=0, two distinct types of uncoupled modes are propagating. This can be seen from (3) and (12):

- H_z, E_r and E_ϕ belong to the field of TM modes,
- whereas E_z, H_r and H_ϕ make up the field of the TE modes.

Finally, comparing the two factors at the left side of (20) with (3.12) and (3.23), shows that these factors correspond to the dispersion equation of the TM and TE modes, respectively. Equations (5), (6), (9) and (10) also show that the field expressions of an axial surface wave tend toward those of a plane surface wave in the limit case of propagation along an electrically extremely thick cylinder.

4.3 Field Distribution of Axial Surface Waves along a Coated, Electric Perfectly Conducting Cylinder

Because of the oscillatory behaviour of the Bessel functions J_n and Y_n, there will be m roots of equation (19) for any given n value. These roots are designated by β_{nm} and the corresponding modes are either TM_{0m}, TE_{0m}, EH_{nm} or HE_{nm} [4, p. 41-42].

As was already suggested towards the end of the previous section, TM and TE modes have no angular dependence, i.e. n=0.

The EH_{11} (or HE_{11}) mode is the fundamental mode; it has no low-frequency cutoff [6, p. 769].

Figure 4.2 shows the transverse electric field vectors in medium 1 for the four lowest order modes.

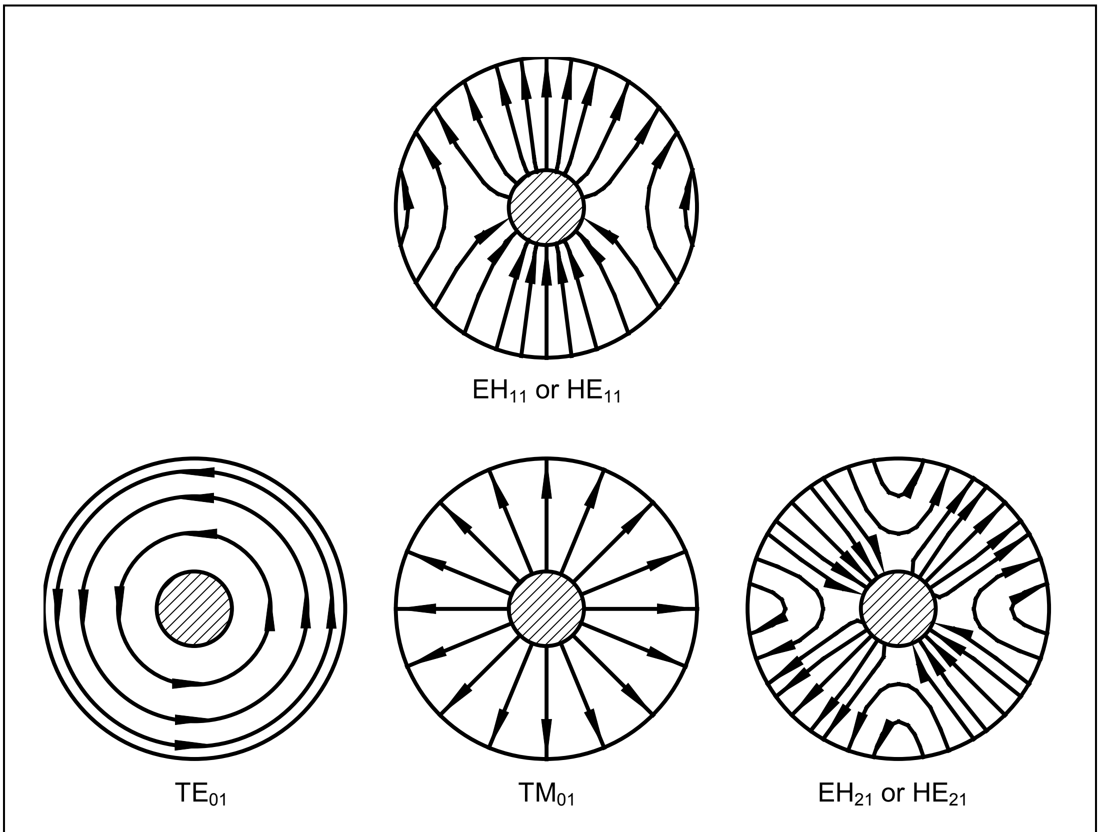

Figure 4.2: The transverse electric field in medium 1 of the four lowest order modes

The external field of a TM axial surface wave is depicted in Figure 4.3. For a TE wave the E- and H-fields are interchanged and one of the fields is reversed in sign.

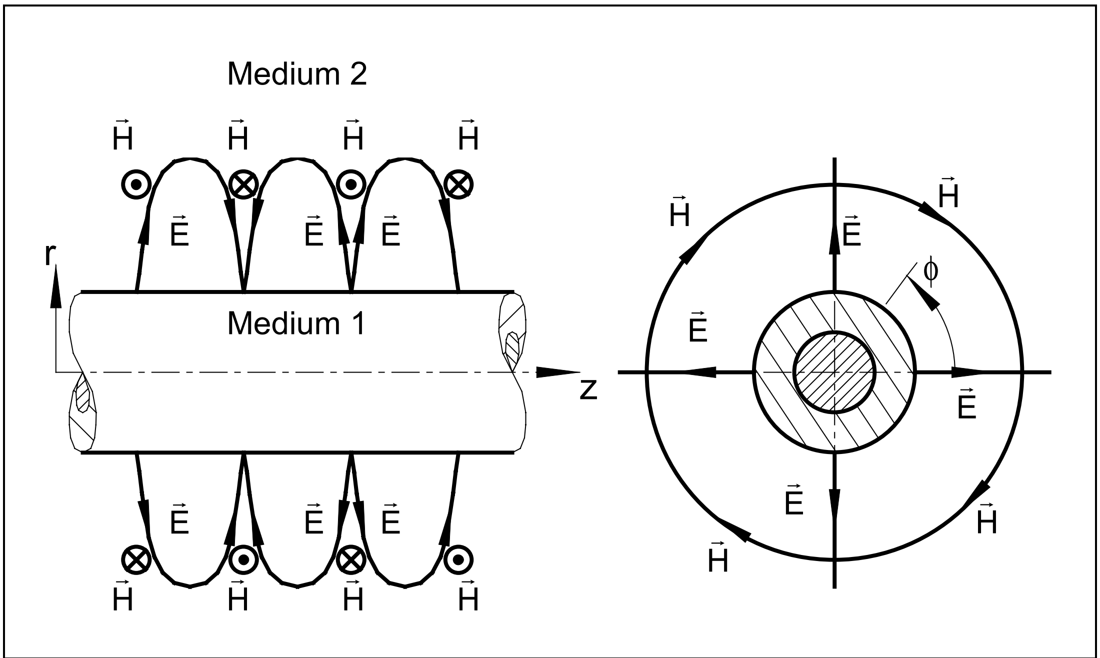

Figure 4.3: The external field of a TM axial surface wave

4.4 Conclusions

Axial surface waves are important because they may be the cause of some significant contributions to the RCS of an aircraft. Axial surface waves can for example propagate along the body of a coated missile.

There are three types of axial wave modes: TM, TE and hybrid. Axial surface waves differ in this respect from plane surface waves that only come in two types: TM (E-type) and TE (H-type).

4.5 References

[1] H. M. Barlow and A. L. Cullen, "Surface waves," *Proceedings of the Institution of Electrical Engineers*, Vol. 100, Part III, No. 68, Nov. 1953, pp. 329-347

[2] H. M. Barlow and J. Brown, *Radio Surface Waves*, Oxford University Press, 1962, p. 12

[3] F. J. Zucker, "Surface-wave antennas," Chapter 12 in R. C. Johnson, *Antenna Engineering Handbook*, McGraw-Hill, 3rd Ed., 1993

[4] G. Keiser, *Optical Fiber Communications*, McGraw-Hill, 2nd Ed.

[5] R. E. Collin, *Field Theory of Guided Waves*, IEEE Press, 2nd Ed., 1991

[6] K. Simonyi, *Theoretische Elektrotechnik*, Johann Ambrosius Barth, 10. Auflage, 1993, (in German)

[7] M. Abramowitz and I. A. Stegun, *Handbook of Mathematical Functions*, Dover Publications,1st Ed., 8th Printing ,1972, p. 359